Nonlinear analysis of concrete-filled thin-walled steel box columns with local buckling effects

Qing Quan Liang[a,*], Brian Uy[b], J. Y. Richard Liew[c]

[a] *School of Civil and Environmental Engineering, The University of New South Wales, Sydney, NSW 2052, Australia*
[b] *School of Civil, Mining and Environmental Engineering, The University of Wollongong, Wollongong, NSW 2522, Australia*
[c] *Department of Civil Engineering, National University of Singapore, Singapore 117576, Singapore*

Abstract

Local buckling of steel plates reduces the ultimate loads of concrete-filled thin-walled steel box columns under axial compression. The effects of local buckling have not been considered in advanced analysis methods that lead to the overestimates of the ultimate loads of composite columns and frames. This paper presents a nonlinear fiber element analysis method for predicting the ultimate strengths and behavior of short concrete-filled thin-walled steel box columns with local buckling effects. The fiber element method considers nonlinear constitutive models for confined concrete and structural steel. Effective width formulas for steel plates with geometric imperfections and residual stresses are incorporated in the fiber element analysis program to account for local buckling effects. The progressive local and post-local buckling is simulated by gradually redistributing the normal stresses within the steel plates. Two performance indices are proposed for evaluating the section and ductility performance of concrete-filled steel box columns. The computational technique developed is used to investigate the effects of the width-to-thickness ratios and concrete compressive strengths on the ultimate strength and ductility of concrete-filled steel box columns. It is demonstrated that the nonlinear fiber element method developed predicts well the ultimate

loads and behavior of concrete-filled thin-walled steel box columns and can be implemented into advanced analysis programs for the nonlinear analysis of composite frames.

Keywords: Composite column; Effective width; Fiber element method; Local buckling; Nonlinear analysis; Strength; Ductility.

---

* Corresponding author. Tel.: +61 2 9385 5062; Fax: +61 2 9385 6139.

E-mail address: q.liang@unsw.edu.au (Q. Q. Liang)

Nomenclature

A_c	total concrete area of a composite cross section
$A_{c,j}$	area of the concrete fiber j
A_{se}	total effective steel area of a composite cross section
$A_{s,i}$	area of the steel fiber i
$A_{u,i}$	area of the steel fiber i at the ultimate load
$A_{u,j}$	area of the concrete fiber j at the ultimate load
b	inner width of a steel box column
b_e	effective width of a steel plate
b_{ne}	ineffective width of a steel plate
$b_{ne,\max}$	maximum ineffective width of a steel plate
B	outer width of a steel box column
D	outer depth of a steel box column

d	inner depth of a steel box column
E_c	Young's modulus of concrete
E_s	Young's modulus of steel
$f_c^{'}$	compressive cylinder strength of concrete
f_y	yield strength of steel
f_u	ultimate strength of steel
m_c	number of concrete fibers in the x direction
m_s	number of steel layers through the thickness of steel box wall
n	knee factor that defines the sharpness of the stress-strain curve for steel
nc	total number of concrete fiber elements
ns	total number of steel fiber elements
P	applied load/axial force
$P_{u.\text{fib}}$	ultimate strength of a composite column predicted by the fiber element method
$P_{u.\text{exp}}$	ultimate strength of a composite column obtained from experiments
PI_d	ductility performance index of composite columns
PI_s	section performance index of composite columns
t	thickness of a steel box
α	strength reduction factor of concrete in the post-peak
γ	parameter used to define stress-strain curve for concrete
ε_c	longitudinal compressive concrete strain
$\varepsilon_c^{'}$	compressive concrete strain corresponding to $f_c^{'}$
ε_{cy}	yield strain of a composite column

ε_s longitudinal strain in steel

ε_u ultimate strain in steel

ε_y yield strain in steel

$\varepsilon_{0.95}$ axial strain of composite column when the load falls to 95% of the ultimate load

ν Poisson's ratio

σ_c longitudinal compressive concrete stress

σ_{cb} critical local buckling stress of steel plates with imperfections

$\sigma_{c,j}$ compressive stress in concrete fiber *j*

σ_{cr} elastic local buckling stress of perfect steel plates

σ_s longitudinal stress in steel

$\sigma_{s,i}$ stress in steel fiber *i*

$\sigma_{u,i}$ stress in steel fiber *i* at the ultimate load

$\sigma_{0.7}$ steel stress corresponding to $E_{0.7} = 0.7E_s$

1. Introduction

Concrete-filled steel box columns have been widely used as primary axial load-carrying members in high rise buildings, bridges and offshore structures because of their excellent performance, such as high strength, high ductility, large energy absorption capacity and low costs. This type of columns can be constructed using either square or rectangular steel hollow box columns filled with either normal or high strength concrete, as shown in Fig. 1. In a concrete-filled thin-walled steel box column under axial compression, the concrete prevents

inward local buckling and steel plates can only buckle outward locally. This buckling mode leads to an increase in the local buckling strength of steel walls and the ultimate strength of the composite column. The steel box as part of a composite column completely encases the concrete core so that the ductility of the encased concrete can be improved. It also serves as longitudinal reinforcement and permanent formwork for the concrete core, which results in significant savings in materials and labor costs.

Experimental studies on concrete-filled steel tubular columns have been conducted. Furlong [1] carried out tests on the ultimate strengths of short concrete-filled steel tube columns. His test results indicated that the axial load was resisted by the steel and concrete components independently and there was no increase in the ultimate strengths of composite columns due to concrete confinement. In addition, the local buckling strength of a steel box filled with concrete was much higher than that of the hollow one. Knowles and Park [2] tested circular and square concrete-filed steel box columns. Their results showed that the circular steel tube offered confinement to the concrete core and the confinement increased the ultimate loads of the columns. The increase in ultimate loads due to confinement effects was observed only in short circular columns. No confinement effect on the ultimate loads, however, was observed in concrete-filled square and rectangular steel box columns. The section shape effects on the ultimate loads of concrete-filled steel stub columns were investigated by Tomii et al. [3]. Their studies demonstrated that concrete confinement was observed in the concrete-filled circular and octagonal steel columns except square columns. Furthermore, Shakir-Khalil and Mouli [4] and Schneider [5] have investigated the experimental ultimate loads and behavior of concrete-filled steel tubular columns.

The ultimate loads and behavior of concrete-filled thin-walled steel box columns are affected

by the local buckling of the steel box walls. Ge and Usami [6,7] presented experimental and analytical studies on the local buckling of concrete-filled steel box columns with and without internal stiffeners. Wright [8,9] used an energy method to derive limiting width-to-thickness ratios for proportioning thin steel plates in contact with concrete. Experimental investigations on the ultimate strengths of concrete-filled steel box columns with local buckling effects have been conducted by Uy and Bradford [10], Bridge et al. [11] and Uy [12]. In addition, Liang and Uy [13,14] proposed effective width models for steel plates in concrete-filled thin-walled steel box columns. These effective width formulas can be used in the determination of the ultimate strengths of composite columns. Moreover, Liang et al. [15,16] proposed buckling and ultimate strength interaction equations for the design of steel plates in double skin composite panels.

Nonlinear analysis methods for steel-concrete composite columns have been reported in the literature. El-Tawil et al. [17] presented an analytical procedure based on the fiber element method for modeling the inelastic behavior of concrete-encased composite columns under axial and biaxial loads. Numerical analysis of concrete-encased composite columns based on the finite difference method was reported by Munoz and Hsu [18]. El-Tawil and Deierlein [19] investigated the strength and ductility of concrete-encased composite columns using the nonlinear fiber element analysis. Lakshmi and Shanmugam [20] presented a semi-analytical method for predicting the behavior of concrete-filled steel box columns. The current state of the art of nonlinear analysis of steel-concrete composite structures was reviewed by Spacone and El-Tawil [21]. The effects of local buckling of steel elements, however, are not considered in most nonlinear analysis methods for concrete-filled steel tubular columns and frames [22]. This is mainly due to the complexity of local buckling of steel elements, which is a function of the state of stresses, plate width-to-thickness ratios, initial geometric

imperfections, residual stresses and boundary conditions. Consequently, the nonlinear analysis methods that do not account for local buckling effects would lead to overestimates of the ultimate loads of composite columns and frames.

The use of high strength concrete in concrete-filled steel box columns increases the ultimate strengths of composite columns but reduces the ductility of the columns because of the brittle nature of high strength concrete. There is a need for a computational technique that can be used to quantify the strength and ductility performance of concrete-filled steel box columns. This paper presents a nonlinear fiber element method for predicting the strength and ductility performance of concrete-filled thin-walled steel box columns with local buckling effects. By adopting the effective width models, the effects of local buckling on the strength and ductility of composite columns are taken into account in the nonlinear fiber element analysis. The progressive local and post-local buckling is simulated by gradually redistributing the normal stresses within the steel box. The effects of plate width-to-thickness ratios and concrete compressive strengths on the structural performance of concrete-filled steel box columns are studied using the proposed fiber analysis method and performance indices. The accuracy of the nonlinear fiber element analysis method is established by comparisons with existing experimental results.

2. Fiber element analysis

2.1 Fiber element discretization

In the fiber element analysis of a concrete-filled steel box column, the composite section is discretized into many small regions (fibers), as depicted in Fig. 2. In the present fiber element

program, the steel wall is divided into m_s layers through its thickness and the discretization of fibers along the width of the wall is automatically undertaken based on the layer size of the wall. The concrete core is divided into m_c fibers in the *x* direction and the size of fibers in the *y* direction is automatically adjusted according to the size of fibers in the *x* direction. The discretization of the cross section results in square fiber elements. Steel fibers are grouped together as well as concrete fibers. Each fiber element in the section can be assigned either concrete or structural steel material properties.

2.2 Material models for structural steel

In the fiber element analysis, fiber stresses are calculated from fiber strains. For a composite section under axial compression, steel and concrete fibers are subjected to the same longitudinal strain. The constitutive models are based on the uniaxial stress-strain relationships of materials. The steel section can be made by mild steel or high strength and cold-formed steels. For mild structural steels, an idealized trilinear stress-strain relationship is employed in the nonlinear fiber element analysis, as shown in Fig. 3. For high strength and cold-formed steels, the stress-strain behavior is characterized by a rounded stress-strain curve. The material model suggested by Ramberg-Osgood [23] is adopted in the fiber element program to calculate fiber stresses for high strength and cold formed steels. The Ramberg-Osgood formula is expressed by

$$\varepsilon_s = \frac{\sigma_s}{E_s}\left[1+\frac{3}{7}\left(\frac{\sigma_s}{\sigma_{0.7}}\right)^n\right] \tag{1}$$

where σ_s is the longitudinal stress in steel, ε_s is the longitudinal strain in steel, E_s is the

Young's modulus of steel, $\sigma_{0.7}$ is the stress corresponding to $E_{0.7} = 0.7E_s$, and *n* is the knee factor that defines the sharpness of the stress-strain curve. The knee factor *n* = 25 is used in the fiber element program to account for the isotropic strain hardening of steel sections [14]. Since the yield stress and strain of structural steel are usually known, $\sigma_{0.7}$ can be determined by substituting the yield stress and strain into Eq. (1). For a given fiber strain, the corresponding fiber stress can be determined from Eq. (1) using numerical procedures.

2.3 Material models for concrete

The elastic-plastic material behavior of compressive concrete is modeled by empirical equations in the fiber element method. It is assumed that the confinement effect increases only the ductility of the concrete in concrete-filled steel box columns but not its strength as suggested by Tomii and Sakino [24]. The general stress-strain curve for concrete in concrete-filled steel box columns is depicted in Fig. 4. The part OA of the stress-strain curve is modeled using the equation suggested by Mander et al. [25] as

$$\sigma_c = \frac{f_c^{'}\gamma\left(\varepsilon_c / \varepsilon_c^{'}\right)}{\gamma - 1 + \left(\varepsilon_c / \varepsilon_c^{'}\right)^{\gamma}} \tag{2}$$

where σ_c is the longitudinal compressive concrete stress, $f_c^{'}$ is the compressive cylinder strength of concrete, ε_c is the longitudinal compressive concrete strain, $\varepsilon_c^{'}$ is the strain at $f_c^{'}$. The parameter γ is defined by

$$\gamma = \frac{E_c}{E_c - \left(f_c^{'} / \varepsilon_c^{'}\right)} \tag{3}$$

where E_c is the Young's modulus of concrete, which is calculated by [26]

$$E_c = 3320\sqrt{f_c^{'}} + 6900 \quad \text{(MPa)} \tag{4}$$

The strain $\varepsilon_c^{'}$ is taken as 0.002 for concrete strength under 28 MPa and 0.003 for concrete strength over 82 MPa. When the concrete strength is between 28 and 82 MPa, the strain $\varepsilon_c^{'}$ is determined as a linear function of the concrete strength.

The parts AB, BC, CD of the stress-strain curve for confined concrete are defined as follows:

$$\sigma_c = f_c^{'} \text{ for } \varepsilon_c^{'} < \varepsilon_c \le 0.005 \tag{5}$$

$$\sigma_c = \alpha f_c^{'} + 100(0.015 - \varepsilon_c)\left(f_c^{'} - \alpha f_c^{'}\right) \text{ for } 0.005 < \varepsilon_c \le 0.015 \tag{6}$$

$$\sigma_c = \alpha f_c^{'} \text{ for } \varepsilon_c > 0.015 \tag{7}$$

where α is equal to 1.0 when the width-to-thickness ratio (*B/t*) of the composite column is less than 24 and it is taken as 0.0 when the width-to-thickness ratio is greater than 64 [24]. For *B/t* ratios between 24 and 64, α is taken as 0.6 in the fiber element analysis program.

2.4 Critical local buckling

Local buckling of thin steel plates in concrete-filled steel box columns under axial compression occurs when the applied load reaches the critical buckling load. Local buckling causes reductions in the strength and stiffness of concrete-filled steel box columns. Fig. 5 shows the effects of local buckling on the load-axial strain behavior of a concrete-filled steel

box column (NS14 in Table 2) predicted by the proposed nonlinear fiber element method. When local buckling of the steel box was not considered, the fiber element method overestimated the ultimate load of the composite column by 10%. Therefore, it is important to account for local buckling effects in the nonlinear analysis of concrete-filled steel tubular columns specially those made of high strength steels and normal concrete in order to predict the true behavior of composite columns.

Local buckling of steel plates in concrete-filled steel box columns is influenced by the width-to-thickness ratios, boundary conditions, initial geometric imperfections and residual stresses induced by welding or cold-formed process [14]. For perfect steel plates, the critical elastic buckling stress can be determined by the following equation [27]

$$\sigma_{cr} = \frac{k\pi^2 E_s}{12\left(1-\nu^2\right)(b/t)^2} \tag{8}$$

where b is the width of the plate, t is the thickness of the plate, ν is the Poisson's ratio and k is the elastic buckling coefficient, which accounts for the effect of the plate aspect ratio and boundary condition on the critical buckling stress. It can be assumed that steel plates in concrete-filled steel box columns are clamped at its four edges as suggested by Wright [8] and Liang and Uy [14]. The minimum elastic local buckling coefficient of 9.81 is used in Eq. (8) in the fiber element analysis program for steel plates in concrete-filled thin-walled steel box columns as suggested by Liang [28].

The critical local buckling stress (σ_{cb}) of steel plates with initial geometric imperfections and residual stresses is much less than that of perfect plates as reported by Liang and Uy [14]. The

critical local buckling stresses of steel plates incorporating the initial out-of-plane deflection of $0.1t$ and residual compressive stress of $0.25f_y$ are approximately evaluated in the proposed fiber element method based on the results obtained from the nonlinear finite element analyses by Liang and Uy [14]. It is assumed that very stocky steel plates can attain the full plastic strength without local buckling effects.

2.5 Post-local buckling

After initial local buckling, thin steel plates are still capable of carrying increased loads without failure. This behavior of thin steel plates is called post-local buckling. The study conducted by Liang and Uy [14] demonstrated that the post-local buckling reserve strength of a clamped steel plate with a *b/t* ratio of 100 was 55 percent of its ultimate strength. Post-local buckling is characterized by the stress redistribution within the buckled steel plate under axial compression. In the post-local buckling regime, the unloaded edge strips of a plate are highly stressed while the heavily buckled central region carries relatively lower stresses. The post-local buckling strength of thin steel plates can be approximately expressed by the effective width concept as illustrated in Fig. 6. It is assumed that at the ultimate state, effective steel fibers are stressed to the yield strength of the steel section while the stresses of ineffective steel fibers are zero. Effective width formulas proposed by Liang and Uy [14] are incorporated in the fiber element analysis program to determine the post-local buckling strength of steel plates in concrete-filled thin-walled steel box columns.

The effective width (b_e) of a plate in axial compression is expressed by

$$\frac{b_e}{b} = 0.675\left(\frac{\sigma_{cr}}{f_y}\right)^{1/3} \quad \text{for } \sigma_{cr} \le f_y \tag{9}$$

$$\frac{b_e}{b} = 0.915\left(\frac{\sigma_{cr}}{\sigma_{cr} + f_y}\right)^{1/3} \quad \text{for } \sigma_{cr} > f_y \tag{10}$$

The above effective width formulas account for the initial out-of-plane defection of $0.1t$ and residual compressive stress of $0.25f_y$.

In the nonlinear analysis, the progressive local and post-local buckling of steel plates in concrete-filled steel box columns is simulated in the fiber element analysis method by gradually redistributing the normal stresses within the steel plates. After the critical local buckling, the ineffective width of a steel plate increases from zero to a maximum value when the applied load is increased to the ultimate load of the steel plate as shown in Fig. 6. The maximum ineffective width of a steel plate corresponding to its ultimate load can be calculated by

$$b_{ne,\max} = b - b_e \tag{11}$$

The ineffective width of the steel plate between zero to $b_{ne,\max}$ can be approximately determined using linear interpolation based on the stress levels of steel fibers as

$$b_{ne} = \left(\frac{\sigma_s - \sigma_{cb}}{f_y - \sigma_{cb}}\right) b_{ne,\max} \tag{12}$$

where σ_{cb} is the critical local buckling stress of a steel plate with initial geometric imperfections and residual stresses. It is noted that the effective width determined by Eq. (9) or Eq. (10) is an ultimate strength criterion that governs the ultimate strength of a steel plate. The ultimate load calculated for the steel plate at any loading stage must not be greater than that determined using the effective width formulas. This implies that if $\sigma_s (b - b_{ne})t > f_y (b - b_{ne,\max})t$, the steel fiber stresses are reduced using linear interpolation to satisfy the effective width criterion as

$$\sigma_s = \left(\frac{b - b_{ne,\max}}{b - b_{ne}} \right) f_y \tag{13}$$

In the fiber element analysis, fiber stresses are firstly calculated using material models from fiber strains. The fiber element analysis program then checks for local buckling. If steel fiber stresses are greater than the critical buckling stress, the effective width of steel walls is calculated and the stresses of steel fiber elements located within the ineffective width (b_{ne}) of the steel box walls are assigned to a zero value. Steel fiber stresses are updated to satisfy the effective width criterion for the ultimate strength. After the initial local buckling, the ineffective width grows with an increase in the applied load until it reaches the maximum value ($b_{ne,\max}$).

2.6 Stress resultants

The axial force applied to the composite column under axial strain deformation is determined as the stress resultant in the composite section, which is expressed by

$$P = \sum_{i=1}^{ns} \sigma_{s,i} A_{s,i} + \sum_{j=1}^{nc} \sigma_{c,j} A_{c,j} \tag{14}$$

where P is the axial load, $\sigma_{s,i}$ is the longitudinal stress at the centroid of steel fiber i, $A_{s,i}$ is the area of steel fiber i, $\sigma_{c,j}$ is longitudinal stress at the centroid of concrete fiber j, $A_{c,j}$ is the area of steel fiber j, ns is the total number of steel fiber elements and nc is the total number of concrete fiber elements. The ultimate strength of a short concrete-filled steel box column is determined as the maximum load in the load-axial strain curve of the composite column.

2.7 Section performance index

It is noted that increasing the steel ratios of composite sections results in the composite sections behaving more like steel sections. In contrast, increasing the compressive concrete strength results in the composite sections behaving more like concrete sections. In the LRFD code [29], a column is classified as composite if it has a structural steel area to the cross-sectional area ratio of more than 0.04 otherwise it is treated as a concrete column. This criterion does not consider the material strengths. El-Tawil and Deierlein [19] suggested a steel contribution ratio, which is defined as the ratio of the steel section strength to the composite section strength to be a better criterion for classification of composite encased columns. Eurocode 4 [30] requires the steel contribution ratio greater than 0.2 for composite columns. A confinement factor was given by Han [31] but it does not take into account of the effect of *b/t* ratios on the behavior of composite sections. To evaluate the section performance of composite columns, a performance index is proposed here as

$$PI_s = \frac{\sum_{i=1}^{ns} \sigma_{u,i} A_{s,i}}{\sum_{j=1}^{nc} \sigma_{u,j} A_{c,j}} \tag{15}$$

where $\sigma_{u,i}$ is the longitudinal stress of steel fiber *i* at the ultimate load and $\sigma_{u,j}$ the longitudinal stress of concrete fiber *j* at the ultimate load. Eq. (15) can be used in the nonlinear fiber element analysis to determine the section performance of composite columns. For simple estimation, the section performance index can be written as

$$PI_s = \frac{f_y A_{se}}{0.85 f_c^{'} A_c} \tag{16}$$

where A_{se} is the total effective steel area of the cross-section and A_c is the total concrete area of the cross-section. The total effective steel area is determined using the effective width formulas. The section performance index proposed accounts for the effects of cross-sectional areas and material strengths of steel and concrete and *b/t* ratios on the behavior of composite sections.

2.8 Ductility performance index

The ductility of a composite section is the ability to undergo large plastic deformations without significant degradations in its strength when subjected to high loads. Ductility is an important performance criterion that must be considered in the performance-based design. The curvature ductility index of a composite section was defined as the ratio of the curvature

at failure to the curvature at yield [19, 32]. To evaluate the ductility performance of concrete-filled thin-walled steel box columns, the ductility performance index is defined as

$$PI_d = \frac{\varepsilon_{0.95}}{\varepsilon_y} \tag{17}$$

where $\varepsilon_{0.95}$ is the axial strain when the load falls to 95% of the ultimate load and ε_y is the axial strain when the composite section is at yield. The axial strain ε_y is approximately defined as the strain when the load attains 95% of the ultimate load. The ductility performance index so defined characterizes the plateau of the load-axial strain curves of composite sections.

3. Validations of the fiber element method

3.1 Load-axial strain curves

To verify the nonlinear fiber element analysis method proposed for analyzing concrete-filled steel box columns with local buckling effects, the load-axial strain curves predicted by the fiber element analysis are compared with experimental results presented by Schneider [5] in this section. Material properties of test specimens are given in Table 1. All steel boxes of the specimens were cold-formed carbon steel and were seam welded and annealed to relieve residual stresses. In the fiber element analysis, the Ramberg-Osgood material model was employed for cold-formed steel sections. Experiments indicated that the maximum compressive stress of concrete in columns varies from $0.85f_c^{'}$ to$1.0f_c^{'}$ [33-36]. This is due to the difference between concrete in a test cylinder and a column, the variation in the concrete

compaction, water-cement ratio and curing conditions and the differences in loading rates between cylinder and column tests. In the present fiber element analysis, the maximum concrete compressive stress in the constitutive model was taken as $1.0 f_c^{'}$ for columns S1, S3, R1, R2 and R3 and $0.85 f_c^{'}$ for specimen S2.

The load-axial strain curves of concrete-filled steel box columns predicted by the proposed fiber element method are compared with experimental results in Figs. 7-12. It can be seen from these figures that the proposed fiber element analysis program predicted very well the axial stiffness, ultimate strengths and post-peak behavior of test specimens. The mean predicted ultimate load for all specimens is 97% of the experimental results. It demonstrates that the nonlinear fiber element method presented is capable of capturing the complete load-axial strain behavior of concrete-filled steel box columns with local buckling effects.

3.2 Ultimate strength

The ultimate strengths of concrete-filled thin-walled steel box columns predicted by the proposed nonlinear fiber element analysis method are compared with experimental results reported by Shakir-Khalil and Mouli [4], Bridge et al. [11] and Uy [37] in Table 2. The load was applied to the steel plates only in the test of specimens B5-B29, NS5, NS11 and NS17 to investigate the local buckling characteristics of steel plates that formed concrete-filled steel box columns. The maximum concrete compressive stress in the constitutive model was taken as $0.85 f_c^{'}$ for specimens in the fiber element analysis. It is seen from Table 2 that the mean ultimate strength of all specimens predicted using the fiber element analysis program is 95.6% of the experimental value. It can be concluded that the proposed fiber element analysis

method is reliable and conservative in predicting the ultimate strengths of concrete-filled thin-walled steel box columns with local buckling effects.

4. Strength and ductility of composite columns

4.1 Effects of width-to-thickness ratios

The ultimate strength and ductility of a concrete-filled steel box column are influenced by the width-to-thickness ratios of the steel box as part of the composite column. Thick steel boxes offer significant confinement to the encased concrete so that the ductility of the confined concrete is increased. In contrast, thin steel boxes are subjected to local buckling that reduces the ultimate strength and confinement effect of composite columns. The proposed fiber element method was used to quantify the effects of width-to-thickness ratios on the ultimate strength and ductility of concrete-filled steel box columns. The thickness of the composite column NS14 shown in Table 2 was varied to give different width-to-thickness ratios for the same size composite section. The *B/t* ratios of these columns were 25.5, 30.6, 38.25, 51 and 102. The maximum compressive concrete strength of $0.85f_c^{'}$ was specified in the analysis.

Fig. 13 shows the effects of *B/t* ratios on the load-axial strain curves of concrete-filled steel box columns. It can be seen from Fig. 13 that the ultimate load and axial stiffness of the concrete-filled steel box column increase with a decrease in the *B/t* ratio for the same size composite section. The section performance index of these composite columns is presented in Fig. 14. The section performance of the concrete-filled steel box column appears to decrease with an increase in its *B/t* ratio. The section performance index decreases from 1.25 to 0.166 when the *B/t* ratio of the composite section increases from 25.5 to 102. Fig. 15 demonstrates

that increasing the width-to-thickness ratio of the section results in a reduction in the ductility performance of the composite column. The composite section with a *B/t* ratio of 25.5 has a performance index of 6.24, which is much higher than that of the section with a *B/t* ratio of 102. The results show that the section performance index also indicates the ductility performance of concrete-filled steel box columns.

4.2 Effects of concrete compressive strengths

The fiber element analysis program was employed to investigate the effects of concrete compressive strengths on the ultimate strength and ductility of concrete-filled steel box columns. The dimensions of the composite section analyzed were 306×306 mm and the thickness of the steel box was 6 mm. The yield stress and Young's modulus of the steel box were 281 MPa and 200 GPa respectively. The compressive cylinder concrete strengths used in the analysis were 32, 40, 60, 80 and 100 MPa. The maximum compressive concrete strength of $0.85f_c^{'}$ was specified in the material model for concrete. The *b/t* ratio of the steel box walls was 49 so that local buckling effects were considered in the nonlinear analysis.

The effects of concrete compressive strengths on the load-axial strain behavior of concrete-filled steel box columns are demonstrated in Fig. 16. It can be observed from Fig. 16 that the ultimate load of the composite column increases with an increase in the strength of the encased concrete. Composite columns filled with high strength concrete possess higher axial stiffness performance than those filled with normal strength concrete. Fig. 17 depicts the section performance index of the steel box column filled with concrete of different strengths. It is seen that increasing the concrete strength results in a decrease in the section performance of the same composite column. The section performance index of the composite column with

32 MPa concrete is 0.706 whilst it is only 0.226 for the column filled with 100 MPa high strength concrete. The effects of concrete strengths on the ductility performance of concrete-filled steel box columns are demonstrated in Fig. 18. It appears from Fig. 18 that the ductility of the composite column decreases with an increase in the strength of the encased concrete. The ductility index of the composite column with 32 MPa concrete is 5.243 and it is only 2.74 when the high strength concrete of 100 MPa was used.

5. Conclusions

A nonlinear fiber element analysis method has been presented in this paper for predicting the ultimate strengths and behavior of short concrete-filled thin-walled steel box columns with local buckling effects. The confinement effect on the ductility of the encased concrete in concrete-filled steel box columns is considered in the method. Effective width formulas proposed for steel plates in concrete-filled steel box columns with geometric imperfections and residual stresses are incorporated in the fiber element method to account for local bucking effects. The fiber element analysis program simulates the progressive local and post-local buckling by redistributing the normal stresses within the steel plates. Two performance indices have been proposed for evaluating the section and ductility performance of composite columns. The effects of width-to-thickness ratios and compressive concrete strengths on the ultimate load and ductility of concrete-filled steel box columns have been investigated using the proposed fiber element analysis program.

Comparisons of the fiber element analyses with existing experimental results demonstrate that the proposed fiber element analysis program predicts well the ultimate strengths and behavior of concrete-filled steel box columns with local buckling effects. The studies presented

indicate that increasing the width-to-thickness ratios reduces the ultimate strength, axial stiffness, section performance and ductility of the same concrete-filled steel box column. In contrast, increasing the compressive concrete strength increases the ultimate strength and axial stiffness of the concrete-filled steel box column but reduces its section performance and ductility. The proposed procedure for simulating the progressive local and post-local buckling of steel plates can be adopted in the nonlinear fiber element analysis of concrete-filled steel tubular columns under axial load and biaxial bending. The fiber element analysis program presented is a valuable tool for predicting the ultimate strength and ductility of concrete-filled steel box columns and can be directly used in design. It can also be incorporated into advanced analysis programs for the nonlinear analysis of concrete-filled steel tubular beam-columns and composite frames.

Acknowledgements

This work is supported by a discovery project grant provided by the Australian Research Council. The first author is an Australian Postdoctoral Fellow of the Australian Research Council and a Guest Professor at Central South University, China. The financial support is gratefully acknowledged.

References

[1] Furlong RW. Strength of steel-encased concrete beam-columns. Journal of Structural Division, ASCE 1967; 93(5): 113-124.

[2] Knowles RB, Park R. Strength of concrete-filled steel tubular columns. Journal Structural Division, ASCE 1969; 95(12): 2565-2587.

[3] Tomii M, Yoshimura K, Morishita Y. Experimental studies on concrete filled steel tubular stub columns under concentric loading. Proceedings of the International Colloquium on Stability of Structures under Static and Dynamic Loads. 1977; 718-741.

[4] Shakir-Khalil H, Mouli M. Further tests on concrete-filled rectangular hollow-section columns. The Structural Engineer 1990; 68(20): 405-413.

[5] Schneider SP. Axially loaded concrete-filled steel tubes. Journal of Structural Engineering, ASCE 1998; 124(10): 1125-1138.

[6] Ge HB, Usami T. Strength of concrete-filled thin-walled steel box columns: experiments. Journal of Structural Engineering, ASCE 1992; 118(11): 3036-3054.

[7] Ge HB, Usami T. Strength analysis of concrete-filled thin-walled steel box columns. Journal of Constructional Steel Research 1994; 30: 259-281.

[8] Wright HD. Buckling of plates in contact with a rigid medium. The Structural Engineer 1993; 71(12): 209-215.

[9] Wright HD. Local stability of filled and encased steel sections. Journal of Structural Engineering, ASCE 1995; 121(10): 1382-1388,

[10] Uy B, Bradford, MA. Local buckling of thin steel plates in composite construction: experimental and theoretical study. Proc. Instn Civ. Engrs. Structures and Buildings 1995; 110: 426-440.

[11] Bridge RQ, O'Shea MD, Gardner P, Grigson R, Tyrell J. Local buckling of square thin-walled steel tubes with concrete infill. Proceedings of the International Conference on Structural Stability and Design, Sydney, Australia. 1995; 307-314.

[12] Uy B. Strength of concrete-filled steel box columns incorporating local buckling. Journal of Structural Engineering, ASCE 2000; 126(3): 341-352.

[13] Liang QQ, Uy B. Parametric study on the structural behaviour of steel plates in concrete-filled fabricated thin-walled box columns. Advances in Structural Engineering 1998; 2(1): 57-71.

[14] Liang, QQ, Uy B. Theoretical study on the post-local buckling of steel plates in concrete-filled box columns. Computers and Structures 2000; 75(5): 479-490.

[15] Liang, QQ, Uy B, Wright HD, Bradford MA. Local and post-local buckling of double skin composite panels. Proc. Instn Civ. Engrs. Structures and Buildings 2003; 156(2): 111-119.

[16] Liang, QQ, Uy B, Wright HD, Bradford MA. Local buckling of steel plates in double skin composite panels under biaxial compression and shear. Journal of Structural Engineering, ASCE 2004; 130(3): 443-451.

[17] El-Tawil S, Sanz-Picón CF, Deierlein GG. Evaluation of ACI 318 and AISC (LRFD) strength provisions for composite beam-columns. Journal of Constructional Steel Research 1995; 34(1): 103-126.

[18] Muñoz PR, Hsu CTT. Behavior of biaxially loaded concrete-encased composite columns. Journal of Structural Engineering, ASCE 1997; 123(9): 1163-1171.

[19] El-Tawil S, Deierlein GG. Strength and ductility of concrete encased composite columns. Journal of Structural Engineering, ASCE 1999; 125(9): 1009-1019.

[20] Lakshmi B, Shanmugam NE. Nonlinear analysis of in-filled steel-concrete composite columns. Journal of Structural Engineering, ASCE 2002; 128(7): 922-933.

[21] Spacone E, El-Tawil S. Nonlinear analysis of steel-concrete composite structures: state of the art. Journal of Structural Engineering, ASCE 2004; 130(2): 159-168.

[22] Liew JYR, Chen H, Shanmugam NE. Inelastic analysis of steel frames with composite beams. Journal of Structural Engineering, ASCE 2001; 127(2): 194-202.

[23] Ramberg W, Osgood WR. Description of stress-strain curves by three parameters. NACA Technical Note. No. 902, 1943.

[24] Tomii M, Sakino K. Elastic-plastic behavior of concrete filled square steel tubular beam-columns. Trans. Arch. Inst. Japan 1979; 280: 111-120.

[25] Mander JB, Priestly MNJ, Park R. Theoretical stress-strain model for confined concrete. Journal of Structural Engineering, ASCE 1988; 114(8): 1804-1826.

[26] ACI-318. Building Code Requirements for Reinforced concrete. ACI, Detroit, MI, 2002.

[27] Bulson PS. The Stability of Flat Plates. Chatto and Windus, London, 1970.

[28] Liang QQ. Performance-Based Optimization of Structures: Theory and Applications. Spon Press, London, 2005.

[29] LRFD. Load and Resistance Factor Design Specification for Steel Buildings. American Institution of Steel Construction; 1999.

[30] Eurocode 4. Design of composite steel and concrete structures, Part 1.1, general rules and rules for buildings; 1994.

[31] Han LH. Tests on stub columns of concrete-filled RHS sections. Journal of Constructional Steel Research 2002; 58(3): 353-372.

[32] Park R. Evaluation of ductility of structures and structural sub-assemblages from laboratory testing. Bull. of the New Zealand Society for Earthquake Engineering 1989; 22(3): 155-166.

[33] Yong Y, Nour MG, Nawy EG. Behavior of laterally confined high-strength concrete under axial loads. Journal of Structural Engineering, ASCE 1988; 114(ST2): 332-352.

[34] Martinez S, Nilson HN, Slate FO. Spirally reinforced high-strength concrete columns. ACI Structural Journal 1984; 81: 431-442.

[35] Cusson D, Paultre P. High-strength concrete columns confined by rectangular ties. Journal of Structural Engineering, ASCE 1994; 120(3): 783-804.

[36] Collins MP, Mitchell D, MacGregor JG. Structural design considerations for high-strength concrete. Concrete International 1993; 27-34.

[37] Uy B. Local and post-local buckling of concrete filled steel welded box columns. Journal of Constructional Steel Research 1998; 47(1-2): 47-72.

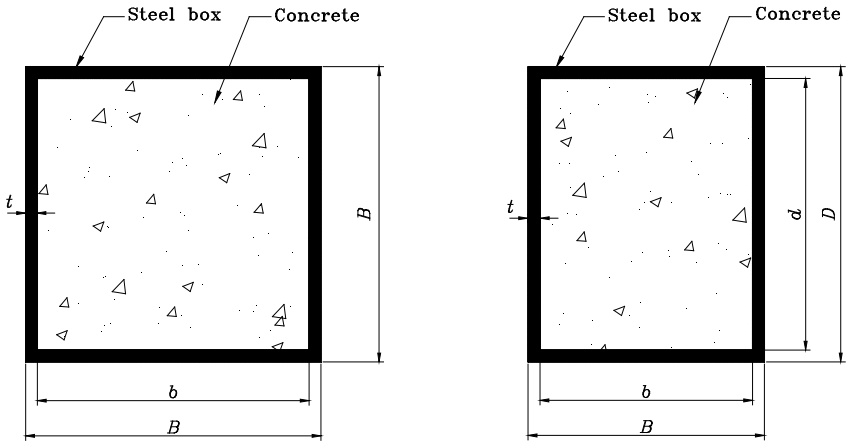

(a) Square section (b) Rectangular section

Fig. 1 Concrete-filled steel box columns

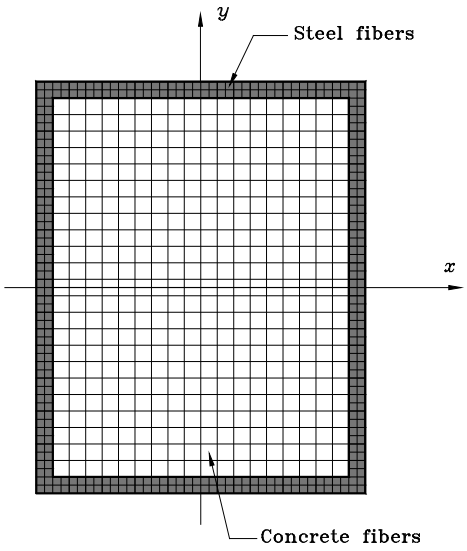

Fig. 2 Fiber element discretization

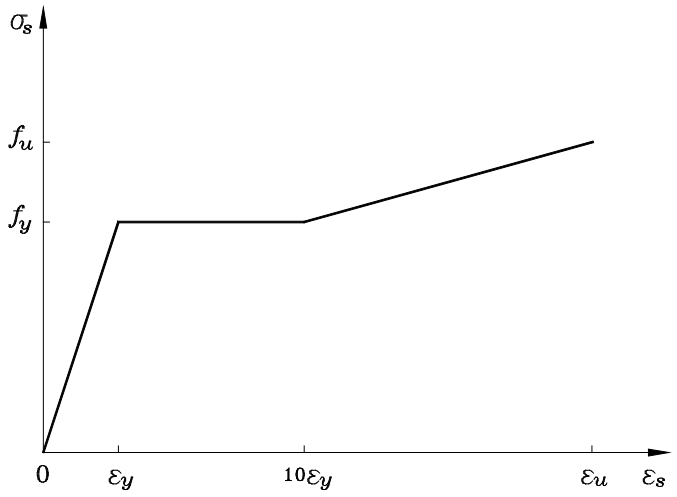

Fig. 3 Idealized stress-strain curve for mild structural steel

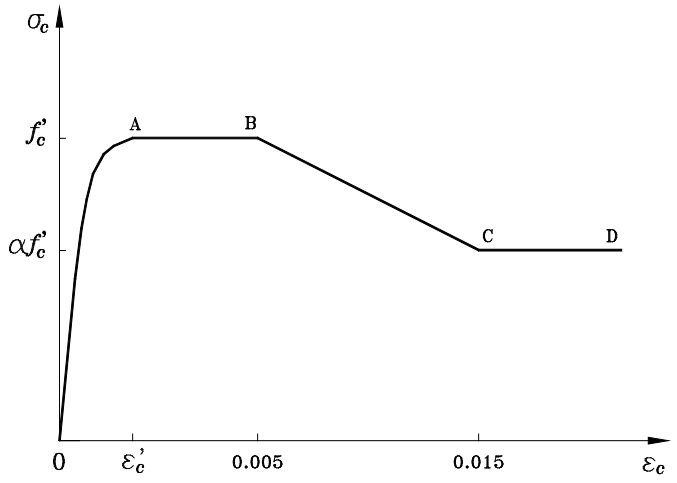

Fig. 4 General stress-strain curve for concrete in concrete-filled steel box columns

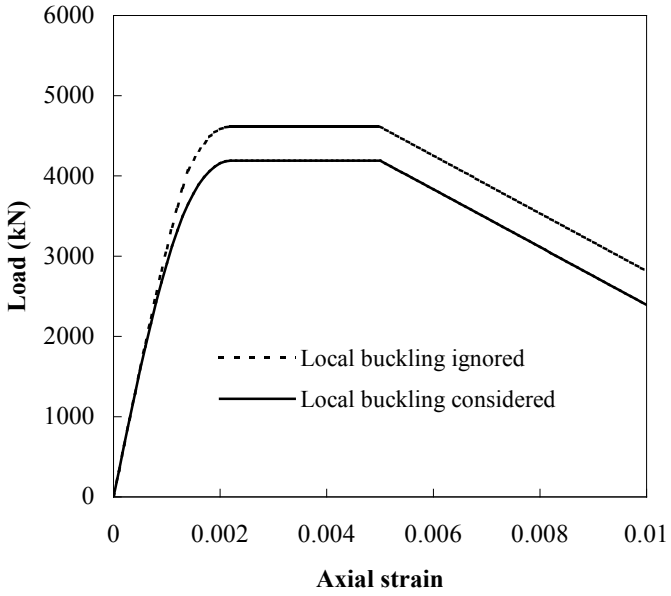

Fig. 5 Effects of local buckling on the performance of concrete-filled steel box columns

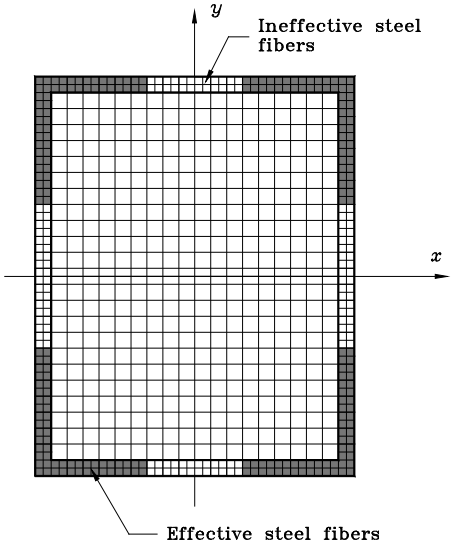

Fig. 6 Effective width of steel plates in concrete-filled steel box column

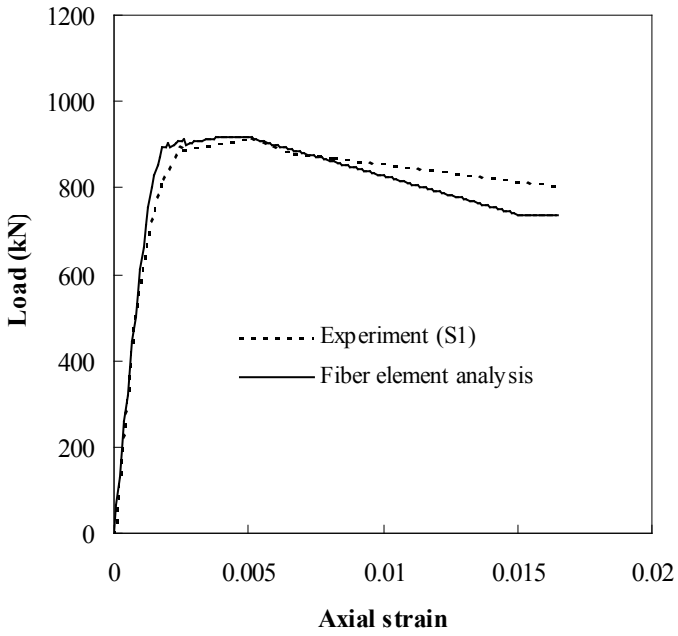

Fig. 7 Comparisons of fiber element analysis with experimental results

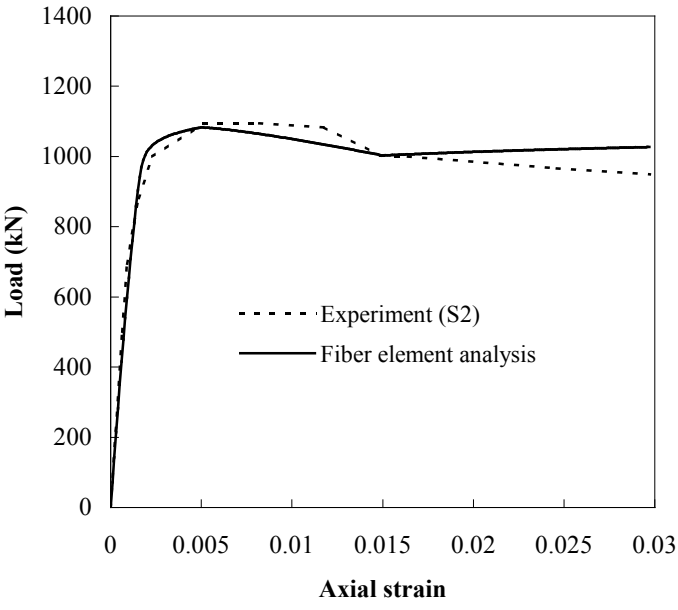

Fig. 8 Comparisons of fiber element analysis with experimental results

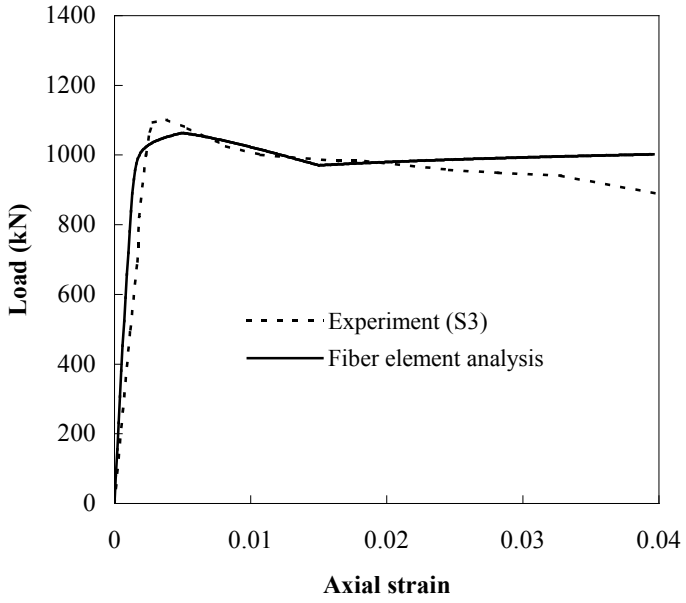

Fig. 9 Comparisons of fiber element analysis with experimental results

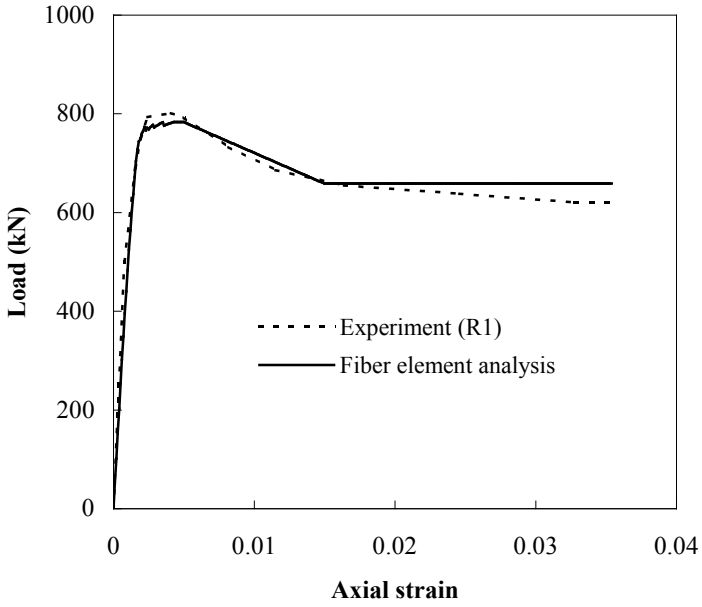

Fig. 10 Comparisons of fiber element analysis with experimental results

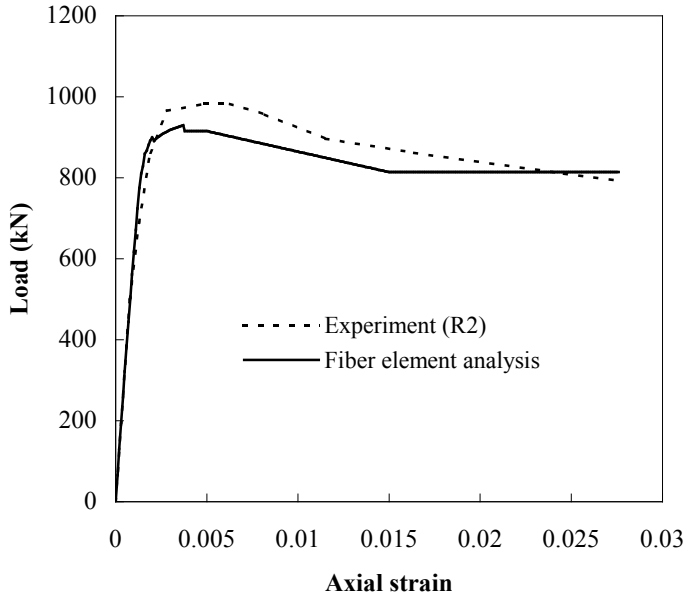

Fig. 11 Comparisons of fiber element analysis with experimental results

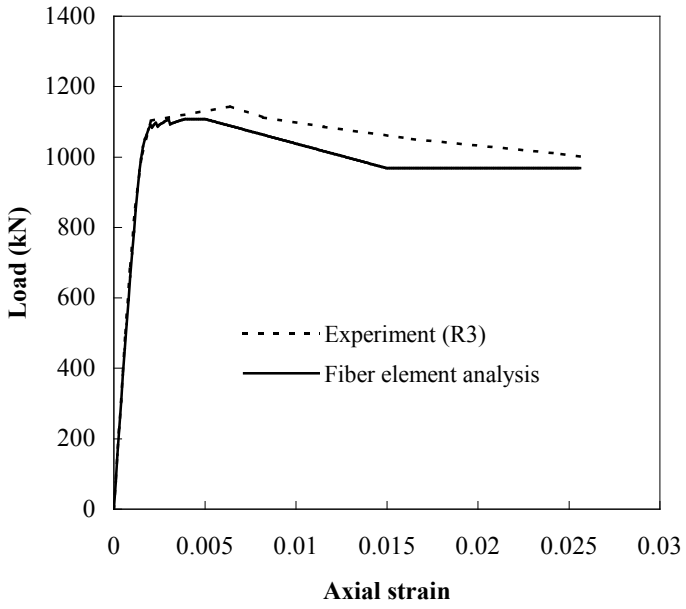

Fig. 12 Comparisons of fiber element analysis with experimental results

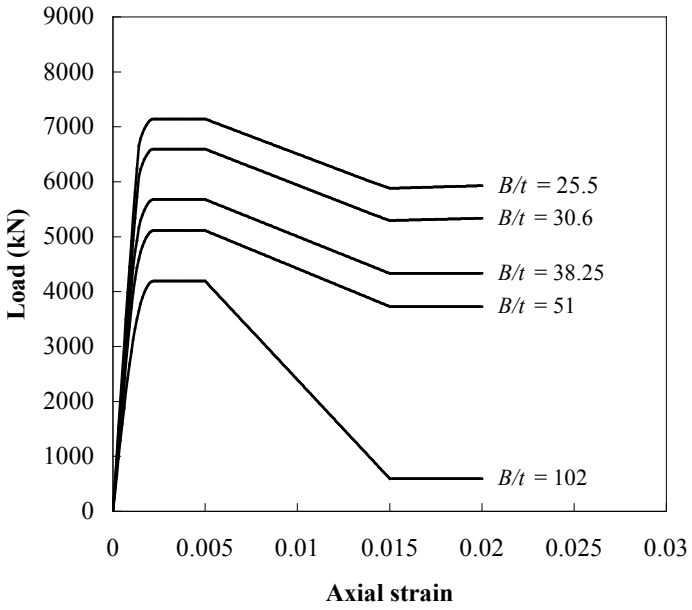

Fig. 13 Effects of *B/t* ratios on the load-axial strain behavior of concrete-filled steel box columns

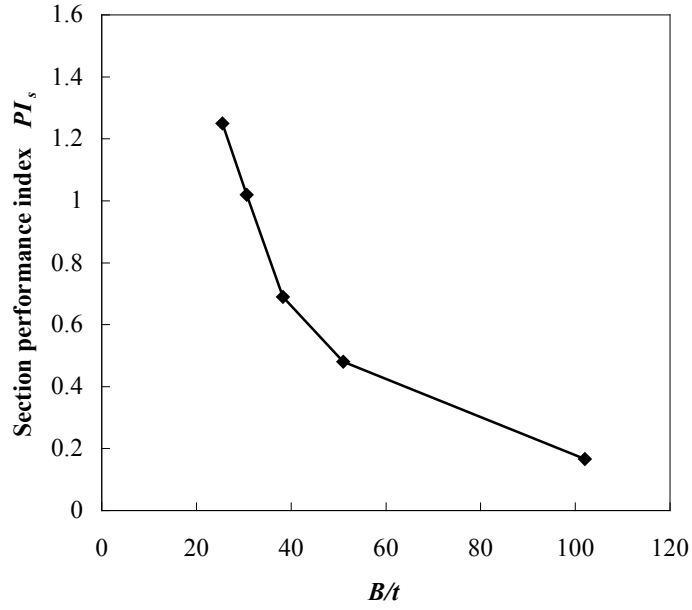

Fig. 14 Effects of *B/t* ratios on the section performance of concrete-filled steel box columns

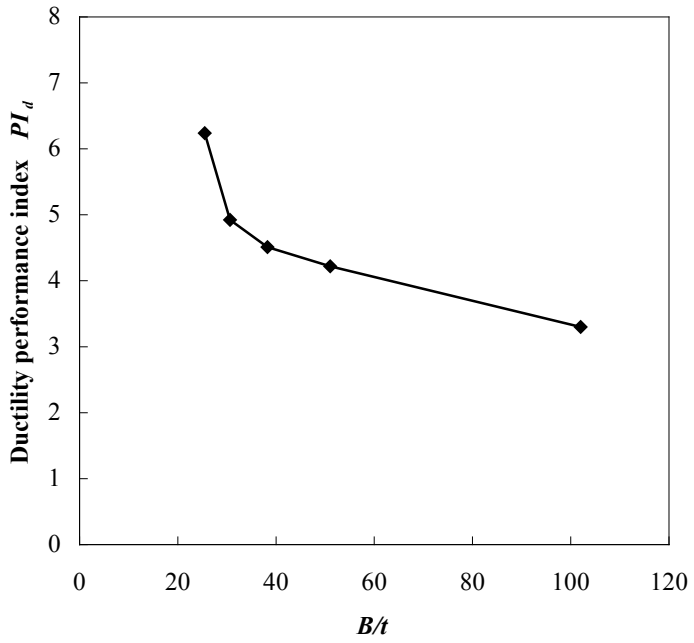

Fig. 15 Effects of *B/t* ratios on the ductility performance of concrete-filled steel box columns

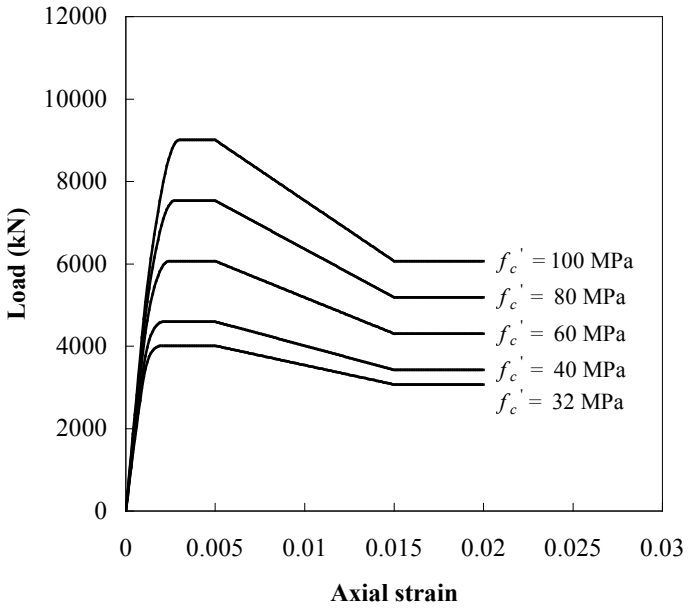

Fig. 16 Effects of concrete strength on the load-axial strain curves of concrete-filled steel box columns

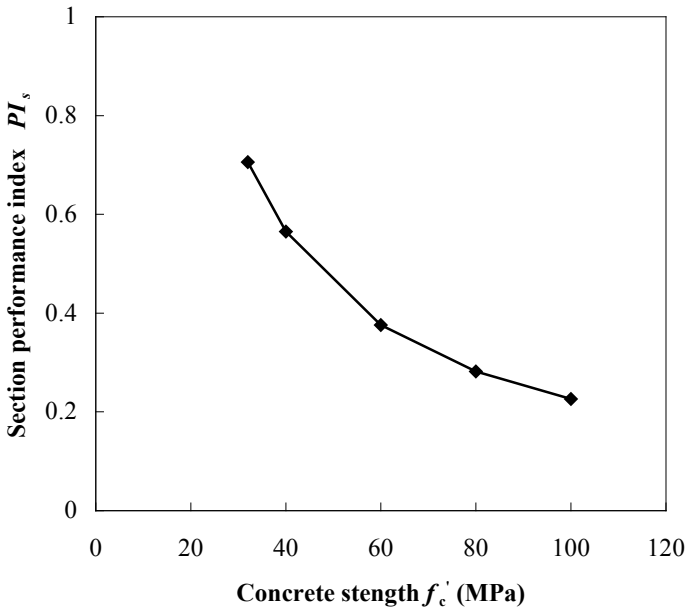

Fig. 17 Effects of concrete strength on the section performance of concrete-filled steel box columns

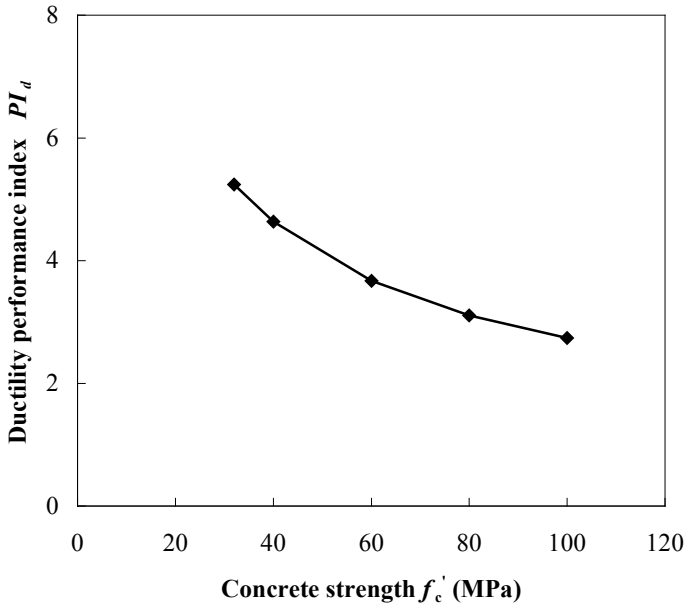

Fig. 18 Effects of concrete strength on the ductility performance of concrete-filled steel box columns

Table 1 Material properties of test specimens

Specimen	$B\times D$ (mm)	t (mm)	f_y (MPa)	E_s (GPa)	$f_c^{'}$ (MPa)
S1	127×127	3.15	356	180.518	30.454
S2	127×127	4.34	357	190.164	26.044
S3	127×127	4.55	322	205.322	23.805
R1	76×152	3.0	430	190.164	30.454
R2	76×152	4.47	383	213.59	26.044
R3	102×152	4.32	413	214.968	26.044

Table 2 Comparisons of fiber element analysis with experimental results

Specimen	$B\times D$ (mm)	t (mm)	f_y (MPa)	E_s (GPa)	$f_c^{'}$ (MPa)	$P_{u.\mathrm{fib}}$ (kN)	$P_{u.\exp}$ (kN)	$\frac{P_{u.\mathrm{fib}}}{P_{u.\exp}}$
B29	282.14×282.14	2.14	282	199.4	—	332	364.2	0.912
B5	202.14×202.14	2.14	282	199.4	—	295.9	311.8	0.949
B20	162.14×162.14	2.14	282	199.4	—	290.3	269	1.079
B17	122.14×122.14	2.14	282	199.4	—	233.8	265.5	0.881
B16	82.14×82.14	2.14	282	199.4	—	167	185	0.903
NS5	186×186	3.0	281	200	—	485.6	517	0.939
NS11	246×246	3.0	292	200	—	567.6	563	1.008
NS17	306×306	3.0	281	200	—	596.8	622.3	0.959
NS1	186×186	3.0	294	200	33.6	1433.4	1555	0.922
NS7	246×246	3.0	292	200	40.6	2555.3	3095	0.826
NS13	306×306	3.0	281	200	44	3962.3	4003	0.99
NS14	306×306	3.0	281	200	47	4192	4253	0.986
NS15	306×306	3.0	281	200	47	4192	4495	0.933
NS16	306×306	3.0	281	200	47	4192	4658	0.90
C1	120×80	5.0	357.5	205	35.7	916.4	850	1.078
C2	120×80	5.0	341	205	38.8	905.8	900	1.006
C3	120×80	5.0	341	205	40.5	916.9	920	0.997
C4	120×80	5.0	362.5	205	39.1	948	950	0.998
C5	120×80	5.0	362.5	205	36	927.7	955	0.971
C6	150×100	5.0	346.7	209.6	38.5	1251.9	1370	0.914
C7	150×100	5.0	346.7	209.6	38.3	1249.7	1340	0.933
C8	150×100	5.0	340	208.6	38.7	1238	1300	0.952
C9	150×100	5.0	340	208.6	39.6	1247.7	1320	0.945
Mean								0.956